Vol 17 No 7, July 2008
1674-1056/2008/17(07)/2600-10

Chinese Physics B

© 2008 Chin. Phys. Soc.
and IOP Publishing Ltd

Solitons and defects in nematic liquid crystals under a simple shear flow and in a static external magnetic field*

Luo Kai-Fu(罗开富)†, Jiang Xiu-Li(蒋秀丽), and Yang Yu-Liang(杨玉良)

Department of Macromolecular Science, Key Laboratory of Molecular Engineering of Polymers of State Ministry Education, Fudan University, Shanghai 200433, *China*

(Received 11 September 2007; revised manuscript received 3 March 2008)

Under a simple shear flow and in a static external magnetic field, the production of defects in the director-aligning regime of nematic liquid crystals has been investigated in terms of the Leslie–Ericksen theory. The equation of motion of the nematic director, which conforms to the driven over-damped sine-Gordon equation, has a soliton solution of the amplitude π. We show that the stationary state with the director uniformly oriented at a Leslie angle is only a metastable state and the potential, which governs the motion of the director, has a number of stable stationary states. For a strong magnetic field, the higher energy barrier between the stable and unstable states leads the director to be locked along the magnetic field direction. However, at the appropriate shear rate and magnetic field the defects, which appear as a stable solitary solution, can be nucleated from a uniformly aligned nematic liquid crystal. We have calculated the stationary travelling velocity of the solitary waves and the distance between a pair of defects.

Keywords: liquid crystals, defects, solitons
PACC: 6130, 6470

1. Introduction

The physics of pattern formation in systems driven far from equilibrium is currently an important subject of the intense theoretical and experimental effort.[1,2] Liquid crystals provide an excellent system to examine nonlinear pattern-forming behaviour.[3,4] Due to the anisotropy of liquid crystal parameters, such as viscosity, elasticity and dielectric susceptibility, several responses of the system to the applied fields appear coupled, resulting in new pattern-forming phenomena. In recent years, a considerable number of studies are carried out on nematic liquid crystals under applied external fields.[5−34]

One extensively studied example is a homeotropically aligned nematic liquid crystal in a continuously rotating magnetic field,[5−10] where many kinds of soliton patterns, such as defect lines,[5] concentric rings,[5,8] lattices of concentric rings[5,8] and spirals,[7] have been observed.

Another interesting example is the instability of the director field in a homeotropically aligned nematic liquid crystal subjected to a shear flow.[11−13] The response of the director to an imposed flow is determined completely by the six Leslie coefficients, $\mu_1 - \mu_6$, and two of them, $\mu_2(< 0)$ and μ_3, are the most important to describe the coupling between flow and director orientation.[4] For $\mu_3 < 0$, a balance of hydrodynamic torques exerted on the director leads to a steady alignment of the liquid crystals at a characteristic angle along the flow direction. For $\mu_3 > 0$, the hydrodynamic torques always tend to rotate the director, resulting in an oscillatory response in material function. We refer to the former situation as flow aligning, while the latter situation as flow tumbling. Nematic liquid crystalline materials under a shear flow are known to exhibit defect production,[14,15] leading to significant concentrations of defect lines. Many transient and stationary patterns are observed during and after the cessation of shear flow. Roll-cells with the roll axis parallel to the flow direction are called stripes and the periodic band textures with the band axis parallel to the vorticity axis are called bands. Under a shear flow, stripes are found experimentally for many polymeric nematic liquid crystals.[16−18] It is generally believed that the stripes only exist in flow-tumbling nematics.[19,20] Band and thread textures are also found during shear,[18,21] especially for the low shear rate and/or the small shear strain.[22,23] On the other hand, after the cessation of shear flow the

*Project supported by the National Natural Science Foundation of China (Grant No 29874011) and State Basic Research Program of China (Grant No 1999064800).
†Corresponding author. E-mail: luokaifu@yahoo.com

patterns are basically the band structure.[18,24,25]

It is generally believed that nematics of the tumbling type should be the candidate for the production of defects[26] due to their propensity for various flow instabilities. However, the situation is not so simple as expected. Surprisingly, it has been found that in initially aligned samples of typical flow-aligning nematic liquid crystals with low molecular weight, such as MBBA[27] and 5CB,[28] a plenty of defects are also produced during the shear flow. This makes unclear the connection between the flow-tumbling nematic liquid crystal and the production of the defect. Furthermore, it has been discovered that in a static external magnetic field, the so-called flow-aligning liquid crystals with $\mu_2/\mu_3 > 0$ can, for an appropriate field strength and direction, exhibit tumbling under a simple shear flow, whereas the original flow-tumbling liquid crystals with $\mu_2/\mu_3 < 0$ can show aligning in a strong magnetic field.[35] Recently, we have discussed solitons and defects in flow-aligning nematic liquid crystals under a simple shear flow.[36] In this work, we further discuss the more complicated case of the system under a simple shear flow and a static external magnetic field.

2. Stability of uniform stationary states

The geometry of the experimental sample is a slab of a nematic liquid crystal of thickness d confined between two parallel glass plates. As shown in Fig.1, a simple shear flow is applied to the system with the flow velocity $\boldsymbol{v}$ in the x direction and the velocity gradient in the y direction, i.e., $v_x = \dot{\gamma} y$, where $\dot{\gamma}$ is the shear rate. Under the generally accepted assumption that the director $\boldsymbol{n}$ always lies in the $x-y$ plane, the orientation of the director is described by θ made with the y-axis. Although this is not the case experimentally, as noted by Gleeson *et al*[37] the essential physics remains the same. In addition, a static external magnetic field with angle $\theta_{\rm h}$ made with the y-axis is also exerted on the system.

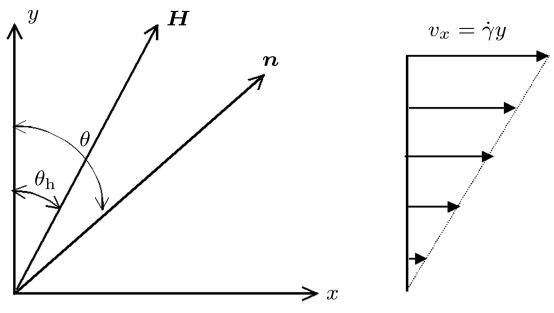


Fig.1. The definition of the coordinate system.

Because we are only interested in the spatial structure in the y direction, it is assumed that the system is uniform along the x direction. The one-dimensional approximation holds true, when the sample thickness d is much larger than the boundary layer of the cell. In the one elastic constant approximation, the dynamic equation of the director orientation is[35−40]

$$\gamma_1 \frac{\partial \theta}{\partial t} = K \frac{\partial^2 \theta}{\partial y^2} + \left(\mu_3 \sin^2\theta - \mu_2 \cos^2\theta\right)\dot{\gamma} - \varepsilon_{\rm h} \sin 2\left(\theta - \theta_{\rm h}\right). \quad (1)$$

Here, K is the Frank's elastic constant, and $\gamma_1 = \mu_3 - \mu_2 > 0$ the rotational or twist viscosity, where μ_2 and μ_3 are two Leslie coefficients. The third term on the right hand of Eq.(1) refers to the maximum magnetic energy for a given magnetic field strength H with $\varepsilon_{\rm h} = 0.5\chi_{\rm a}H^2$, where $\chi_{\rm a}$ is the anisotropy of the magnetic susceptibility and is, without loss of generality, assumed to be positive. For $\varepsilon_{\rm h} = 0$, the dynamic equation under a simple shear flow is recovered. For $\dot{\gamma} y$ lower than the velocity of the soliton, we have $\partial\theta/\partial t + \dot{\gamma} y \partial\theta/\partial x \approx \partial\theta/\partial t$. Thus, we can also obtain the same results in the x direction.

As in Refs.[35–40], the linear velocity profile in the flow direction is assumed. This is not the case in reality, as the liquid crystalline systems can have strongly non-Newtonian flow properties. In principle, the Navier–Stoke equation should be coupled with appropriate boundary conditions. This is very complicated and cannot be solved analytically. However, numerically the assumption on v_x has been checked to be valid.[37]

We should note in advance that Eq.(1) conforms to the driven over-damped sine-Gordon equation[41]

$$\kappa \frac{\partial^2 \theta}{\partial x^2} - \gamma \frac{\partial \theta}{\partial t} + F - V_0 \sin\theta = 0, \quad (2)$$

where V_0 is the maximum potential and F the driving force. The driven over-damped sine-Gordon equation has a solution of stable propagating soliton of amplitude 2π.[41] Thus, the complex spatial structures could exist in the nematic liquid crystals.

For a uniform system,

$$\gamma_1 \frac{\partial \theta}{\partial t} = \left(\mu_3 \sin^2\theta - \mu_2 \cos^2\theta\right)\dot{\gamma} - \varepsilon_{\rm h} \sin\left(2\left(\theta - \theta_{\rm h}\right)\right). \quad (3)$$

Equation (3) reveals that there exist two kinds of solutions, i.e., director aligning and director tumbling types.

In the director-aligning regime, there exist two stationary solutions, which are obtained by solving the following equation:

$$\left(\mu_3 \sin^2\theta - \mu_2 \cos^2\theta\right)\dot{\gamma} - \varepsilon_{\rm h} \sin\left(2\left(\theta - \theta_{\rm h}\right)\right) = 0. \quad (4)$$

The necessary and sufficient condition for director aligning is

$$\mu_3\mu_2 - (\mu_3 + \mu_2)\, S_{\rm h} \sin(2\theta_{\rm h}) + S_{\rm h}^2 > 0, \quad (5)$$

where $S_{\rm h} = \varepsilon_{\rm h}/\dot{\gamma} = 0.5\chi_{\rm a}H^2/\dot{\gamma}$, indicating the effective field strength relative to the shear rate. Based on Eq.(5), we obtain the diagram for director tumbling and director aligning in a static magnetic field, as shown in Fig.2.[35] In a static magnetic field, the

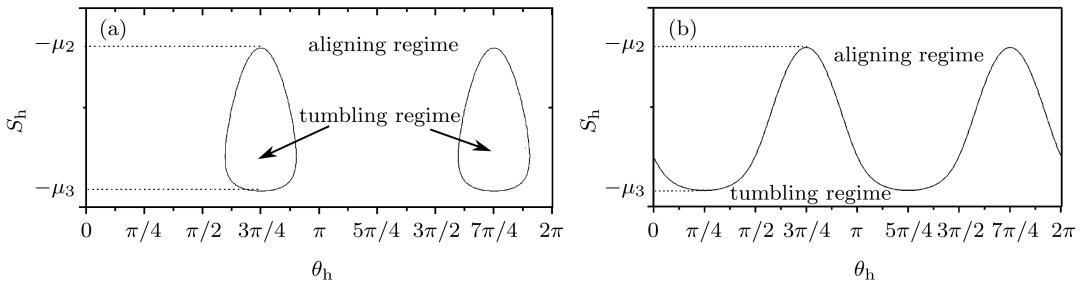


Fig.2. State diagrams for the original aligning-type (a) and the tumbling-type (b) of nematic liquid crystals subject to a simple shear flow and a static magnetic field (see also in Ref.[5]).

so-called flow-aligning liquid crystal with $\mu_3 < 0$ can, for the appropriate field strength and direction, exhibit tumbling, whereas the original flow-tumbling liquid crystal with $\mu_3 > 0$ can show aligning.[35] For the non-stationary state, Eq.(3) describes a time-dependent director motion of a uniform system. In the director-tumbling regime, both theoretical analysis[35] and Brownian dynamics simulations[42–44] have shown that the director is continuously rotating with time with a well-defined time period.

In the director-aligning regime, Eq.(4) has a set of stable stationary solutions $\theta_{\rm s}$ and a set of unstable ones $\theta_{\rm u}$. The linear stability analysis shows

$$\theta_{\rm s} = k\pi + \arctan\left(\frac{-S_{\rm h}\cos(2\theta_{\rm h}) + \sqrt{\mu_3\mu_2 - (\mu_3+\mu_2)\, S_{\rm h}\sin(2\theta_{\rm h}) + S_{\rm h}^2}}{S_{\rm h}\sin(2\theta_{\rm h}) - \mu_3}\right) \quad (6)$$

and

$$\theta_{\rm u} = k\pi + \arctan\left(\frac{-S_{\rm h}\cos(2\theta_{\rm h}) - \sqrt{\mu_3\mu_2 - (\mu_3+\mu_2)\, S_{\rm h}\sin(2\theta_{\rm h}) + S_{\rm h}^2}}{S_{\rm h}\sin(2\theta_{\rm h}) - \mu_3}\right), \quad (7)$$

where k is an integer. For $S_{\rm h} \to \infty$, Eqs.(6) and (7) give $\theta_{\rm s} \to k\pi + \theta_{\rm h}$ and $\theta_{\rm u} \to k\pi + \pi/2 - \theta_{\rm h}$. In the next section, we will see that the so-called stable stationary states are only metastable.

3. Spatial inhomogeneity

In order to analyse the possibility, structure and the conditions for the onset of spatial structures, the strategy of Ref.[41] will be closely followed.

3.1. Potential energy

The motion of the director described by Eq.(1) can also be written as

$$\gamma_1 \frac{\partial \theta}{\partial t} = -\frac{\delta E(\theta)}{\delta \theta},$$

where the energy functional, which governs the director motion, is

$$E(\theta) = \int {\rm d}y \left[V(\theta) + \frac{K}{2}\left(\frac{\partial \theta}{\partial y}\right)^2\right], \quad (8)$$

with potential energy density

$$V(\theta) = -\frac{\dot{\gamma}}{2}(\mu_3 - \mu_2)\theta + \frac{\dot{\gamma}}{4}(\mu_3 + \mu_2)\sin(2\theta) - \frac{\varepsilon_\mathrm{h}}{2}\cos(2(\theta - \theta_\mathrm{h})). \quad (9)$$

As shown in Fig.3, $V(\theta)$ has stationary points given by Eqs.(6) and (7). In numerical calculations, we have set $\mu_2 = -0.4$ and $\mu_3 = -0.04$.

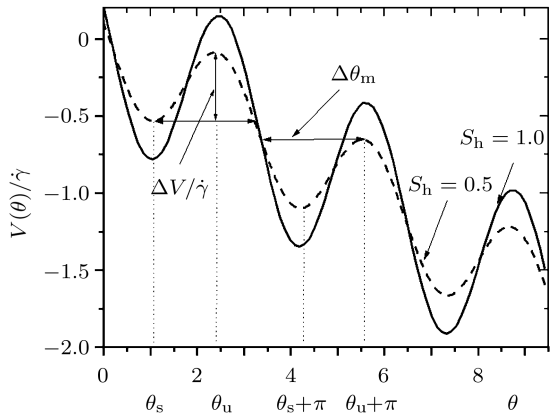


Fig.3. The potential $V(\theta)$ for $S_\mathrm{h} = 0.25, 1.0$ with $\mu_2 = -0.4, \mu_3 = -0.04$ and $\theta_\mathrm{h} = 1$. The angles θ_s and θ_u denote the stable and unstable stationary states. The maximum deviation from θ_s is labelled as $\Delta\theta_\mathrm{m}$. ΔV is the potential energy barrier between the state of $\theta_{s,k}$ and the next stationary state, $\theta_{s,k+1}$.

The energy density difference between stable and unstable stationary states, ΔV, which is the energy barrier for the system to transfer from a stable stationary state to the next unstable stationary state, is written as

$$\Delta V = V(\theta_\mathrm{u}) - V(\theta_\mathrm{s}) = -\frac{\dot{\gamma}}{2}(\mu_3 - \mu_2)(\theta_\mathrm{u} - \theta_\mathrm{s}) + \dot{\gamma}\sqrt{\mu_3\mu_2 - (\mu_3 + \mu_2)\,S_\mathrm{h}\sin(2\theta_\mathrm{h}) + S_\mathrm{h}^2}. \quad (10)$$

When the second term on the right hand side of Eq.(10) is the leading term compared with the first term, the energy barrier is very high. Hence the liquid crystal director is locked along the magnetic field direction. However, we should point out that the energy barrier for the system of $\theta_{s,k}$ to climb up to the next hill of $\theta_{u,k+1}$ and transfer to the next minimum of $\theta_{s,k+1}$ is low for appropriate S_h, θ_h and $\dot{\gamma}$. Therefore, the thermal fluctuation and/or the mechanical noises should be able to lead the system to sequentially transfer to the lower valleys.

In Fig.3, if all the director is aligned in the stationary state of $\theta_{s,k}$, the potential of state k is higher than the state $k+1$, i.e., with $\theta_{s,k+1} = \theta_{s,k} + \pi$. Due to the fact that the reduced potential, $V(\theta)/\dot{\gamma}$, has infinite stationary states, there can be states in which θ increases monotonically, undergoing more or less discrete changes π at each pair of defects. Although we know that nematic liquid crystals have the property of $\boldsymbol{n} = -\boldsymbol{n}$, and their energy should be the same if all the nematic liquid crystalline molecules have rotated an angle of π; here the reduced potential energy $V(\theta)/\dot{\gamma}$ simply implies that the states of certain $\theta_{s,k}$ $(k = 0, 1, 2, \ldots)$ are only metastable, and thus the fluctuation-assisted transition of the system from one minimum to the next one will be most likely to occur through a time sequence of configurations requiring the minimum intermediate elevation in energy. If one block of the directors in the middle of the system are rotated by an angle of π, i.e. it has been transferred to the stationary state of $\theta_{s,k+1}$, while all the others are staying in the stationary state of $\theta_{s,k}$, then one pair of defects is generated. We should notice here that the term of defect is widely used in the literature of liquid crystals, while it is termed as kink and antikink by Büttiker and Landauer[41] or in the literatures of condensed state physics.[45] The fact is that the block which has rotated an angle of π has gained the potential energy which can compensate the energy costs for generating defect pairs. Therefore, the balance between the gained potential energy and the energy for producing of defects determines the number of defects. As the states of $\theta_{s,k}$ is only metastable, there should exist saddle points. In order to know the director configurations when the system starts to transfer, we have to search for the saddle points in the energy surface $E(\theta)$ through which the director configuration can pass.[41]

3.2. Nucleus for the spatial inhomogeneity

It is clear that the saddle points in the energy surface are given by the solution of

$$-\frac{\delta E(\theta)}{\delta\theta} = K\frac{\mathrm{d}^2\theta}{\mathrm{d}y^2} + \frac{1}{2}(\mu_3 - \mu_2)\dot{\gamma} - \frac{1}{2}(\mu_3 + \mu_2)\dot{\gamma}\cos(2\theta) - \varepsilon_\mathrm{h}\sin(2(\theta - \theta_\mathrm{h})) = 0. \quad (11)$$

Multiplying with $\mathrm{d}\theta/\mathrm{d}y$ and integrating it, we obtain

$$K\left(\frac{\mathrm{d}\theta}{\mathrm{d}y}\right)^2 - 2V(\theta) = 2U_0, \quad (12)$$

where U_0 is integration constant.

To determine the value of U_0 we assume that the system stays in a certain uniform state with $\theta = \theta_\alpha$ initially, thus we have $(\mathrm{d}\theta/\mathrm{d}y)|_{y=0} = 0$ and $V(\theta) = V(\theta_\alpha)$. This results in $U_0 = -V(\theta_\alpha)$. Then, from Eq.(11), with $U_0 = -V(\theta_\alpha)$, the excess energy of the critical nucleus from the uniform initial state θ_α is given by

$$\Delta E_{N,\alpha} = \Delta E(\theta_\alpha) = K \int \left(\frac{\mathrm{d}\theta}{\mathrm{d}y}\right)^2 \mathrm{d}y. \qquad (13)$$

First, we discuss the case of $\theta_\alpha \neq \theta_\mathrm{s} \neq \theta_\mathrm{u}$. After introducing the deviation from the state θ_α, i.e., $\Delta\theta(y) = \theta(y) - \theta_\alpha$, and substituting into Eq.(12) with $U_0 = -V(\theta_\alpha)$, we obtain

$$\begin{aligned} & K\left(\frac{\mathrm{d}\Delta\theta}{\mathrm{d}y}\right)^2 \\ = & -\dot{\gamma}\left(\mu_3 - \mu_2\right)\Delta\theta + \frac{1}{2}\dot{\gamma}\left(\mu_3 + \mu_2\right)\cos(2\theta_\alpha)\sin(2\Delta\theta) \\ & + \frac{1}{2}\dot{\gamma}\left(\mu_3 + \mu_2\right)\sin(2\theta_\alpha)\left(\cos(2\Delta\theta) - 1\right) \\ & - \varepsilon_\mathrm{h}\cos(2\left(\theta_\alpha - \theta_\mathrm{h}\right))\left(\cos(2\Delta\theta) - 1\right) \\ & + \varepsilon_\mathrm{h}\sin(2\left(\theta_\alpha - \theta_\mathrm{h}\right))\sin(2\Delta\theta). \end{aligned} \qquad (14)$$

The formal solution is

$$\begin{aligned} & \int \mathrm{d}(\Delta\theta)\Big[- \left(\mu_3 - \mu_2\right)\Delta\theta \\ & + \frac{1}{2}\left(\mu_3 + \mu_2\right)\cos(2\theta_\alpha)\sin(2\Delta\theta) \\ & + \frac{1}{2}\left(\mu_3 + \mu_2\right)\sin(2\theta_\alpha)\left(\cos(2\Delta\theta) - 1\right) \\ & - S_\mathrm{h}\cos(2\left(\theta_\alpha - \theta_\mathrm{h}\right))\left(\cos(2\Delta\theta) - 1\right) \\ & + S_\mathrm{h}\sin(2\left(\theta_\alpha - \theta_\mathrm{h}\right))\sin(2\Delta\theta)\Big]^{-1/2} \\ = & \pm\sqrt{\frac{\dot{\gamma}}{K}}y. \end{aligned} \qquad (15)$$

Equation (15) has been integrated numerically with the boundary condition of $\Delta\theta(y = 0) = \Delta\theta_\mathrm{m}$, and the results are shown in Fig.4. We call this large amplitude nucleus (LAN).

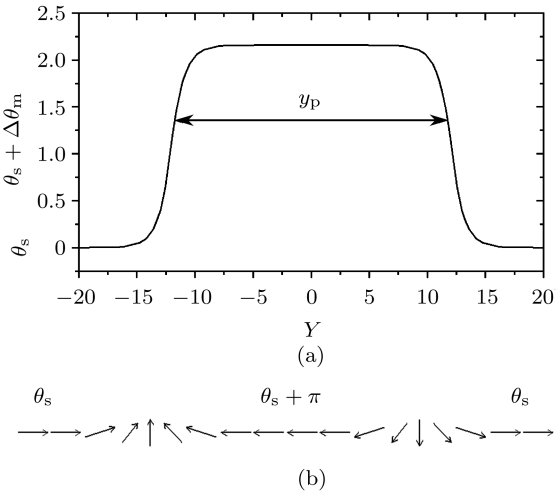


Fig.4. (a) The critical nucleus generated from stationary state θ_s under the boundary condition of $\Delta\theta = \Delta\theta_\mathrm{m}(y = 0)$ and $\Delta\theta = 0(y = \pm d)$, with $S_\mathrm{h} = 0.5$ and $\theta_\mathrm{h} = 1$. In the figure, the reduced length scale is defined as $Y = \sqrt{\frac{\dot{\gamma}}{K}}y$. (b) Schematic drawing of a pair of defects with $\Delta\theta_\mathrm{m} = \pi$. The heads of the arrows do not have physical significance, which only help the reader keep track of the orientation and topology.

In order to discuss the small amplitude nucleus (SAN) of the defect pair, we expand the left side of Eq.(14) into powers of $\Delta\theta$ and only keep the terms up to the order of $\Delta\theta^2$. When $(\mu_3 + \mu_2)\sin(2\theta_\alpha) - 2S_\mathrm{h}\cos(2\left(\theta_\alpha - \theta_\mathrm{h}\right)) > 0$, we obtain

$$\Delta\theta_\mathrm{NP}(y) = \Delta\theta_\mathrm{mP}\left(1 \pm \sin(\Omega y)\right), \qquad (16)$$

with

$$\Delta\theta_\mathrm{mP} = \frac{\left(\mu_3 + \mu_2\right)\cos(2\theta_\alpha) - \left(\mu_3 - \mu_2\right) + 2S_\mathrm{h}\sin(2\left(\theta_\alpha - \theta_\mathrm{h}\right))}{2\left[\left(\mu_3 + \mu_2\right)\sin(2\theta_\alpha) - 2S_\mathrm{h}\cos(2\left(\theta_\alpha - \theta_\mathrm{h}\right))\right]},$$

and

$$\Omega = \sqrt{\frac{\dot{\gamma}\left[\left(\mu_3 + \mu_2\right)\sin(2\theta_\alpha) - 2S_\mathrm{h}\cos(2\left(\theta_\alpha - \theta_\mathrm{h}\right))\right]}{K}}.$$

Here, $(\mu_3 + \mu_2)\sin(2\theta_\alpha) - 2S_\mathrm{h}\cos(2\left(\theta_\alpha - \theta_\mathrm{h}\right)) > 0$ can be fulfilled when θ_α is near θ_u.

When the system is in a uniform state of θ_α, it can be seen from Eq.(16) that the system will leave that uniform state (θ_α) and exhibit the periodic patterns (bands with the axis parallel to the vorticity axis). As this is a periodic structure, it is called periodic nucleus and labelled as $\Delta\theta_\mathrm{NP}(y)$.

It is interesting to note that, when $\theta_\alpha = \theta_\mathrm{s}$ (or $\theta_\alpha = \theta_\mathrm{u}$), the coefficient in front of the term $\Delta\theta$ is zero in the power series expansion of $V(\theta_\mathrm{s} + \Delta\theta)$ (or $V(\theta_\mathrm{u} + \Delta\theta)$). Therefore, we call the director configuration, i.e., the saddle-point configuration emerged from

the stationary states, $\theta_{\rm s}$, critical nucleus and labelled as $\Delta\theta_{\rm NC}(y)$.

To search for the critical nucleus, we can expand the left side of Eq.(15) into powers of the small deviation $\Delta\theta_{\rm NC}$ and keep the terms up to the order of $\Delta\theta_{\rm NC}^3$. We obtain

$$\int {\rm d}(\Delta\theta_{\rm NC}) \left[A\Delta\theta_{\rm NC} + B\Delta\theta_{\rm NC}^2 + C\ \Delta\theta_{\rm NC}^3\right]^{-1/2} = \pm\sqrt{\frac{\dot\gamma}{K}}y, \tag{17}$$

where

$$\begin{aligned} A &= (\mu_3+\mu_2)\cos(2\theta_{\rm s}) - (\mu_3-\mu_2) \\ &\quad +2S_{\rm h}\sin(2\left(\theta_{\rm s}-\theta_{\rm h}\right)) = 0, \\ B &= -\left(\mu_3+\mu_2\right)\sin(2\theta_{\rm s}) + 2S_{\rm h}\cos(2\left(\theta_{\rm s}-\theta_{\rm h}\right)) \\ &= 2\sqrt{\mu_3\mu_2 - \left(\mu_3+\mu_2\right)S_{\rm h}\sin(2\theta_{\rm h}) + S_{\rm h}^2}, \end{aligned}$$

and

$$\begin{aligned} C &= -\frac{2}{3}\left[\left(\mu_3+\mu_2\right)\cos(2\theta_{\rm s}) + 2S_{\rm h}\sin(2\left(\theta_{\rm s}-\theta_{\rm h}\right))\right] \\ &= -\frac{2}{3}\left(\mu_3-\mu_2\right). \end{aligned}$$

We should mention that $-B$ is simply the stability condition of the stationary state and thus B is always positive for the stable stationary state $\theta_{\rm s}$. Then, the solution of the above equation can be written as

$$\Delta\theta_{\rm NC} = \Delta\theta_{\rm mC}\frac{1}{\cosh^2\left(\dfrac{y}{2\xi_{\rm C}}\right)}, \tag{18}$$

with

$$\begin{aligned} \Delta\theta_{\rm mC} &= -\frac{B}{C} \\ &= \frac{3\sqrt{\mu_3\mu_2 - \left(\mu_3+\mu_2\right)S_{\rm h}\sin(2\theta_{\rm h}) + S_{\rm h}^2}}{\left(\mu_3-\mu_2\right)}, \end{aligned}$$

and

$$\xi_{\rm C} = \sqrt{\frac{K}{2\dot\gamma\sqrt{\mu_3\mu_2 - \left(\mu_3+\mu_2\right)S_{\rm h}\sin(2\theta_{\rm h}) + S_{\rm h}^2}}}.$$

Here, we have set $\Delta\theta_{\rm NC}(y=0) = \Delta\theta_{\rm m}$.

Equation (18) is a soliton-like solution which describes a pair of defects separated by a distance of $2\xi_{\rm C}$. Actually, in the limit of $\mu_3 \approx \mu_2$, i.e., $\gamma_1 = \mu_3 - \mu_2 \to 0$, Eq.(14) has a solution of sine-Gordon soliton[41] of amplitude π,

$$\Delta\theta_{\rm S(\pm)} = 2k\pi + 2\arctan\left[\exp\left(\pm\frac{y}{\xi_{\rm s}}\right)\right], \tag{19}$$

with $\xi_{\rm s} = \sqrt{\dfrac{K}{2\dot\gamma\sqrt{\mu_3^2 - 2\mu_3 S_{\rm h}\sin(2\theta_{\rm h}) + S_{\rm h}^2}}}$.

3.3. Domain size

Equation (16) gives the periodicity of the spatial variation of the director, and the characteristic size l of the director fluctuation is

$$l = \pi\sqrt{\frac{K}{\dot\gamma\left[\left(\mu_3+\mu_2\right)\sin(2\theta_\alpha) - 2S_{\rm h}\cos(2\left(\theta_\alpha-\theta_{\rm h}\right))\right]}}.$$

From Eq.(18), the distance of a pair of defects (which is called domain size in the literature of liquid crystals) is

$$l = 2\xi_{\rm C} = 2\sqrt{\frac{K}{2\dot\gamma\sqrt{\mu_3\mu_2 - \left(\mu_3+\mu_2\right)S_{\rm h}\sin(2\theta_{\rm h}) + S_{\rm h}^2}}}.$$

Since we have only expanded the right side of Eq.(14) according to small $\Delta\theta$, the above results are only suitable for the small amplitude nucleus of the defects. To find the distance between a pair of defects of large amplitude as shown in Fig.4, we have to set $\Delta\theta = \Delta\theta_{\rm m} + \phi$, then we obtain

$$\begin{aligned} \frac{K}{\dot\gamma}\left(\frac{{\rm d}\phi}{{\rm d}y}\right)^2 &= B\left(\Delta\theta_{\rm m}+\phi\right)^2 \\ &= \left[-\left(\mu_3+\mu_2\right)\sin(2\theta_{\rm s})\right. \\ &\quad \left.+2S_{\rm h}\cos(2\left(\theta_{\rm s}-\theta_{\rm h}\right))\right]\left(\Delta\theta_{\rm m}+\phi\right)^2. \end{aligned}$$

The above equation describes the exponential behaviour of a pair of defects, which has the solution of $y = \pm\sqrt{\dfrac{K}{B\dot\gamma}}\ln\left(\Delta\theta_{\rm m}+\phi\right)$. From Fig.4, we can see that the top of the director configuration of critical nucleus (a pair of defects) is very flat. To obtain the width of the flat top of the critical configuration, we should extend the above integration to an angle $\phi_{\rm p} \gg \Delta\theta_{\rm m}$, and keep $\phi_{\rm p} \ll \pi$. This is always valid because $\Delta\theta_{\rm m}$ is small as shown in Eq.(18). The flat top of the nucleus (a pair of the defects), therefore, has an extension $2y_{\rm p}$, with $y_{\rm p}$ given by

$$\begin{aligned} & y_{\rm p} \\ &= \pm\sqrt{\frac{K}{B\dot\gamma}}\ln\left(\Delta\theta_{\rm m}+\phi_{\rm p}\right) \approx \pm\sqrt{\frac{K}{B\dot\gamma}}\ln(\Delta\theta_{\rm m}) \\ &= \pm\sqrt{\frac{K}{2\dot\gamma\sqrt{\mu_3\mu_2 - \left(\mu_3+\mu_2\right)S_{\rm h}\sin(2\theta_{\rm h}) + S_{\rm h}^2}}} \\ &\quad \times\ln\frac{3\sqrt{\mu_3\mu_2 - \left(\mu_3+\mu_2\right)S_{\rm h}\sin(2\theta_{\rm h}) + S_{\rm h}^2}}{\left(\mu_3-\mu_2\right)}, \end{aligned} \tag{20}$$

as $\phi_{\rm p}$ is large and makes almost no contribution to $y_{\rm p}$.

3.4. Energy barrier in the production of defects

For the critical nucleus, the energy barrier in its crossing the saddle is $\Delta E_{\rm NC}$. In the limit of small amplitude nucleus, which is the defined by Eq.(18), $\Delta E_{\rm NC}$ can be calculated analytically

$$\Delta E_{\rm NC} = \frac{8}{15}\frac{K\Delta\theta_{\rm mC}^2}{\sqrt{\dfrac{K}{2\dot\gamma\sqrt{\mu_3\mu_2-(\mu_3+\mu_2)\,S_{\rm h}\sin(2\theta_{\rm h})+S_{\rm h}^2}}}} = \frac{24}{5}\frac{\left(\mu_3\mu_2-(\mu_3+\mu_2)\,S_{\rm h}\sin(2\theta_{\rm h})+S_{\rm h}^2\right)^{5/4}}{(\mu_3-\mu_2)^2}\left(2K\dot\gamma\right)^{1/2}.$$

For the case of periodic nucleus, the energy barrier to a pair of defects is

$$\Delta E_{\rm NP} = \frac{\pi}{8}\frac{\left[(\mu_3+\mu_2)\cos(2\theta_\alpha)-(\mu_3-\mu_2)+2S_{\rm h}\sin(2\,(\theta_\alpha-\theta_{\rm h}))\right]^2\left(K\dot\gamma\right)^{1/2}}{\left[(\mu_3+\mu_2)\sin(2\theta_\alpha)-2S_{\rm h}\cos(2\,(\theta_\alpha-\theta_{\rm h}))\right]^{3/2}}.$$

It is seen that the energies of the states $\Delta\theta_{\rm NC}$ and $\Delta\theta_{\rm NP}$, i.e. $\Delta E_{\rm NC}$ and $\Delta E_{\rm NP}$, are stationary with respect to small changes in the director configuration. Here, $\Delta E_{\rm NP}$ becomes very small when $[(\mu_3+\mu_2)\cos(2\theta_\alpha)-(\mu_3-\mu_2)+2S_{\rm h}\sin(2\,(\theta_\alpha-\theta_{\rm h}))]$ is very small. This happens when θ_α is near $\theta_{\rm u}$, indicating that the system will overcome the barrier $\Delta E_{\rm NP}$ easily and the periodic director patterns emerge when the system occasionally passes through the unstable stationary state, $\theta_{\rm u}$.

As $\theta_{\rm s}$ is in the quadrant where $(\mu_3+\mu_2)\sin(2\theta_\alpha)-2S_{\rm h}\cos(2(\theta_\alpha-\theta_{\rm h}))<0$, the fluctuation will leads the system to pass through the saddle, and pairs of defects described by Eq.(18) will be nucleated. However, when $S_{\rm h}$ and $\dot\gamma$ is low, the fluctuation can occasionally lead the system to pass through the potential barrier ΔV described by Eq.(10), especially when ΔV is very small also. The director can either overcome the barrier and transfer to the next minimum of $\theta_{\rm s}$ or, on the way of passing through the potential hill, the fluctuation will lead the system to leave from the potential hill and nucleate the periodic structures described by Eq.(18). We should note in advance that the periodic solution is unstable, therefore, it can only be observed as a transient pattern.

4. The stability of the pattern

According to Eq.(11), the motion equation for $\Delta\theta$ is written as

$$\begin{aligned}\gamma_1\frac{\partial(\Delta\theta)}{\partial t} &= K\frac{\partial^2(\Delta\theta)}{\partial y^2}+\frac{1}{2}\dot\gamma\,(\mu_3-\mu_2)\\ &\quad-\frac{1}{2}\,(\mu_3+\mu_2)\,\dot\gamma\cos(2\theta_\alpha)\cos(2\Delta\theta)\\ &\quad+\frac{1}{2}\,(\mu_3+\mu_2)\,\dot\gamma\sin(2\theta_\alpha)\sin(2\Delta\theta)\\ &\quad-\varepsilon_{\rm h}\cos(2\,(\theta_\alpha-\theta_{\rm h}))\sin(2\Delta\theta)\\ &\quad-\varepsilon_{\rm h}\sin(2\,(\theta_\alpha-\theta_{\rm h}))\cos(2\Delta\theta).\end{aligned}\tag{21}$$

The stationary solution for the above equation has been solved in the last section. Now, we assume another deviation from $\Delta\theta_\alpha(y)$ by an amount of $\delta\theta(y,t)$ and therefore $\Delta\theta(y,t)=\Delta\theta_\alpha(y)+\delta\theta(y,t)$. By expanding to the first order of $\delta\theta(y,t)$ and the first order of $\Delta\theta_\alpha(y)$, we obtain the motion equation for $\delta\theta(y,t)$

$$\begin{aligned}\gamma_1\frac{\partial(\delta\theta)}{\partial t} &= K\frac{\partial^2(\delta\theta)}{\partial y^2}+(\mu_3+\mu_2)\,\dot\gamma\\ &\quad\times\left[2\cos(2\theta_\alpha)\Delta\theta_\alpha+\sin(2\theta_\alpha)\right]\delta\theta\\ &\quad+2\varepsilon_{\rm h}[\cos(2(\theta_\alpha-\theta_{\rm h}))\\ &\quad-2\sin(2(\theta_\alpha-\theta_{\rm h}))\Delta\theta_\alpha]\delta\theta.\end{aligned}\tag{22}$$

As θ_α and $\Delta\theta_\alpha(y)$ are independent of time, the solution of the above equation can be assumed to have the form of

$$\delta\theta(y,t)=\delta\theta(y)\exp\left(-\lambda t\right).\tag{23}$$

Substituting Eq.(23) into Eq.(22) leads to the eigenvalue problem of

$$\mathrm{L}(\delta\theta(y))=-\lambda\gamma_1\delta\theta(y).\tag{24}$$

The operator L is defined as $\mathrm{L}=K\dfrac{\mathrm{d}^2}{\mathrm{d}y^2}+R\left(\theta_\alpha,\Delta\theta_\alpha\right)$ with

$$\begin{aligned}&R\left(\theta_\alpha,\Delta\theta_\alpha\right)\\ &=(\mu_3+\mu_2)\,\dot\gamma\left[2\cos(2\theta_\alpha)\cdot(\Delta\theta_\alpha)+\sin(2\theta_\alpha)\right]\\ &\quad+2\varepsilon_{\rm h}\left[\cos(2\,(\theta_\alpha-\theta_{\rm h}))-2\sin(2\,(\theta_\alpha-\theta_{\rm h}))(\Delta\theta_\alpha)\right].\end{aligned}$$

For the case of critical nucleus, the eigenvalue equation is written as

$$\frac{\mathrm{d}^2(\delta\theta)}{\mathrm{d}y^2}+\left[\left(\frac{\lambda\gamma_1}{K}-\frac{1}{\xi_{\mathrm{C}}^2}\right)+\frac{3}{\xi_{\mathrm{C}}^2\cosh^2\left(\dfrac{y}{2\xi_{\mathrm{C}}}\right)}\right]\delta\theta=0, \tag{25}$$

where ξ_{C} is defined in Eq.(18). Equation (25) is similar to that in the case of single particle moving in a potential. The above eigenvalue equation is similar to the driven and over-damped sine-Gordon equation.[41] The eigenvalue problem of the above equation can be solved following Landau and Lifshitz:[46] the eigenvalues for the localized modes are $\lambda_{\mathrm{n}}^{\mathrm{C}}=\dfrac{K}{\gamma_1\xi_{\mathrm{c}}^2}\left[1-\dfrac{(3-n)^2}{4}\right]$, where $n=0,1$ and 2. The corresponding eigenfunctions are

$$\delta\theta_0^{\mathrm{C}}=C_0(\xi_{\mathrm{C}})\,\mathrm{sec\,h}^3\left(\frac{y}{2\xi_{\mathrm{C}}}\right),$$

$$\delta\theta_1^{\mathrm{C}}=C_1(\xi_{\mathrm{C}})\frac{\sinh\left(\dfrac{y}{2\xi_{\mathrm{C}}}\right)}{\cosh^2\left(\dfrac{y}{2\xi_{\mathrm{C}}}\right)},$$

and

$$\delta\theta_2^{\mathrm{C}}=C_2(\xi_{\mathrm{C}})\frac{1-4\sinh^2\left(\dfrac{y}{2\xi_{\mathrm{C}}}\right)}{\cosh^3\left(\dfrac{y}{2\xi_{\mathrm{C}}}\right)},$$

where C_0, C_1 and C_2 are normalization constants. The unstable mode $\delta\theta_0^{\mathrm{C}}(y)$ with eigenvalue λ_0^{C} describes the contraction or extension of the pair of defects. The second eigenmode $\delta\theta_1^{\mathrm{C}}(y)$ with eigenvalue λ_1^{C} describes the translation of the defect pair. The third eigenmode $\delta\theta_2^{\mathrm{C}}(y)$ with eigenvalue λ_2^{C} describes the extension or contraction of the width of each defect. It is seen that the energy decreases in the direction of the unstable localized eigenmode, $\delta\theta_0^{\mathrm{C}}(y)$, and increases in the stable localized eigenmode $\delta\theta_2^{\mathrm{C}}(y)$. Following the discussion of Büttiker and Landauer,[41] the curvature near the saddle of the energy surface in the direction of a certain mode (n) is proportional to $1/\lambda_n^{\mathrm{C}}$. Therefore, we can see that the saddle of the energy surface in the direction of $\delta\theta_2^{\mathrm{C}}(y)$ is flat and it is very flat in the direction of $\delta\theta_0^{\mathrm{C}}(y)$. This also implies that the production of defects can happen easily.

5. Stability and the travelling velocity of the soliton

Due to the existence of macroscopic shear flow, the drift of the pair of defects will be basically in the flow direction. To investigate the propagation of these driven defects, we search, generally, for the stationary travelling waves $\theta(z)$ which depend on y and t only in the combination $z=y+ut$, where u is the propagation velocity of the defect pair in the minus y direction. For a stationary travelling of the defect pair with velocity u, Eq.(1) becomes

$$\begin{aligned}&K\frac{\partial^2\theta}{\partial z^2}-u\gamma_1\frac{\partial\theta}{\partial z}+\frac{1}{2}(\mu_3-\mu_2)\dot\gamma\\&-\frac{1}{2}(\mu_3+\mu_2)\dot\gamma\cos(2\theta)\\&-\varepsilon_{\mathrm{h}}\sin(2(\theta-\theta_{\mathrm{h}}))=0.\end{aligned} \tag{26}$$

By linearizing Eq.(26) with respect to a small perturbation $\delta\theta(y)$ to soliton $\Delta\theta_{\mathrm{S}}(y)$ of Eq.(19), the motion equation for $\delta\theta(y)$ is

$$\begin{aligned}&K\frac{\partial^2(\delta\theta)}{\partial z^2}-u\gamma_1\frac{\partial(\delta\theta)}{\partial z}-[(\mu_3+\mu_2)\dot\gamma\sin(2\Delta\theta_{\mathrm{s}})\\&+2\varepsilon_{\mathrm{h}}\cos(2(\Delta\theta_{\mathrm{s}}-\theta_{\mathrm{h}}))]\cdot\delta\theta=0.\end{aligned} \tag{27}$$

Actually, for the sine-Gordon soliton described by Eq.(19), it is well known that the travelling of the soliton is stable against the small perturbations.[41,47]

We have numerically analysed the flow of $(\mathrm{d}\theta/\mathrm{d}z,\theta)$ for Eq.(26), as shown in Fig.5, and found

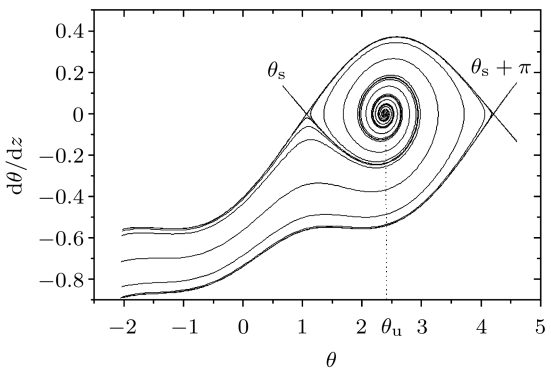


Fig.5. The phase diagram calculated from Eq.(26). For the case of $\mu_2=-0.4$, $\mu_3=-0.04$, it is shown that the travelling defects connect $(0,\theta_{\mathrm{s}})$ with $(0,\theta_{\mathrm{s}}+\pi)$, an unstable solitary solution is emerging from $(0,\theta_{\mathrm{s}})$ and spiraling to $(0,\theta_{\mathrm{u}})$. The unbounded travelling waves can also be seen from the figure.

two types of solutions. The first solitary solution emerges from a stable stationary state $(0,\ \theta_{\rm s})$ and spirals to the neighbouring unstable state $(0,\ \theta_{\rm u})$, which is unstable against small perturbations. This solution corresponds to our solution of periodic nucleus, Eq.(16). The second solitary solution departs from a stable uniform state $\theta_{s,k}$ and approaches the next neighbouring state $\theta_{s,k+1}$. This solution is stable against small perturbations. The flow of $({\rm d}\theta/{\rm d}z, \theta)$ reveals that the critical nucleus generated from the stable state $\theta_{s,k}$ is stable while the periodic nucleus generated from unstable state $\theta_{u,k}$ is unstable. If the system accidentally goes to the unstable state $\theta_{u,k}$ due to some mechanical or other noises, the travelling wave will be spiraling away from that state and get into the stable solution. This character of the flow diagram is coincident with the qualitative discussion given in Section 2. It also agrees with the analysis given by Büttiker and Thomas[47] for the over-damped sine-Gordon soliton.

Fortunately, the travelling velocity of defects, u, can be calculated analytically. Following Ref.[41], we obtain

$$u = \frac{\pi}{4}\sqrt{\frac{K\dot{\gamma}}{\sqrt{(\mu_3+\mu_2)^2 + 4S_{\rm h}^2 - 4S_{\rm h}\,(\mu_3+\mu_2)\sin(2\theta_{\rm h})}}}. \tag{28}$$

We should note that for a given shear rate, when $S_{\rm h} > (\mu_3+\mu_2)\sin(2\theta_{\rm h})$ the static external magnetic field can decrease the travelling velocity. On the contrary, when $S_{\rm h} < (\mu_3+\mu_2)\sin(2\theta_{\rm h})$, the static external magnetic field can increase the travelling velocity. The velocity of the stationary travelling soliton u can also be determined by a numerical method introduced by Büttiker *et al.*[47] The values of u obtained by numerically solving Eq.(26) are shown in Fig.6 and is in excellent agreement with the analytical results, Eq.(28). However, in the limiting case of the strong shear rate and magnetic field, the first two terms on the left side of Eq.(27) can be neglected, thus in flow-aligning regime the system will be uniform with a director angle of $\theta_{\rm s}$.

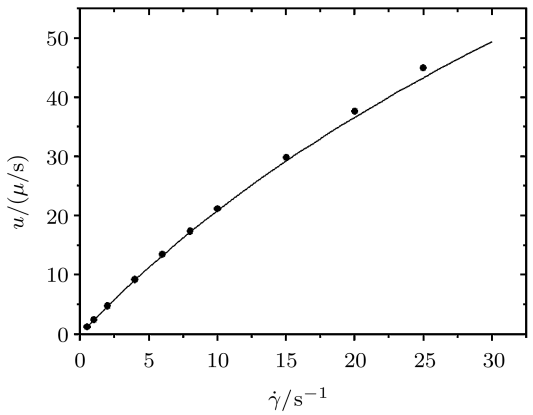


Fig.6. Propagation velocity of a pair of defects as a function of the shear rate. In the calculation, μ_2 and μ_3 have been set to be –0.4 and –0.04, respectively which corresponds to the values of 5CB. The dots are obtained by numerical simulation of Eq.(26) and the solid line is the analytical result of Eq.(28).

6. Summary and conclusions

We have developed the nucleation theory for the production of defects in shear-aligning regime of nematic liquid crystals under a simple shear flow and a static magnetic field. The production of defects is the characteristic behaviour of the director-aligning regime of nematic liquid crystals. When the static external magnetic field is very strong, the energy barrier between the stable and unstable states is very high. But for the appropriate shear rate and also the appropriate strength and direction of the static external magnetic field, the defects, appearing as a stable solitary solution, can be nucleated from a uniformly aligned nematic liquid crystal. It is found that there are two types of spatial patterns, i.e., unstable periodic nucleus and stable critical nucleus. The periodic pattern can be observed at low shear rate and low magnetic field strength. However, the periodic pattern can only be observed as a transient pattern because it is unstable against small disturbances. The spatial pattern can only be formed through critical nucleation of soliton-like structure, i.e., pairs of defects. The distance between a pair of defects, also called the periodicity of the band pattern and the characteristic size of domain, has also been calculated.

References

[1] Wesfreid J, Brand H, Monneville P, Albinet G and Bocara N (editors) 1988 *Propagation in Systems Far from Equilibrium* (Berlin: Springer)

[2] Field R J and Burger M (editors) 1985 *Oscillations and Traveling Wave in Chemical Systems* (New York: Wiley)

[3] Lam L and Prost J (editors) *Solitons in liquid crystals* (New York: Springer-Verlag)
[4] De Gennes P G and Prost J (editors) 1993 *The Physics of Liquid Crystals* (Oxford: Clarendon)
[5] Migler K B and Meyer R B 1991 *Phys. Rev. Lett.* **66** 1485
[6] Migler K B and Meyer R B 1993 *Phys. Rev.* E **48** 1218
[7] Migler K B and Meyer R B 1994 *Physica* D **71** 412
[8] Pashkovsky E E, Stille W, Strobl G and Talebi D 1997 *J. Phys.* II (France) **7** 707
[9] Brochard F 1974 *J. Phys. Lett.* (Paris) **35** L19
[10] Brochard F, Leger L and Meyer R B 1975 *J. Phys.* (Paris) **36** Suppl. C1 209
[11] Pieranski P and Guyon E 1977 *Phys. Rev. Lett.* **39** 1280
[12] Burghardt W R 1991 *J. Rheol.* **35** 49
[13] Burghardt W R and Fuller G G 1990 *J. Rheol.* **34** 959
[14] Graziano D J and Mackley M R 1984 *Mol. Cryst. Liq. Cryst.* **106** 103
[15] Cladis P E and Torza S 1976 *Colloid. Interface Sci.* **4** 487
[16] P Pieranski and Guyon E 1974 *Phys. Rev. Lett.* **32** 924
[17] Larson R G and Mead D W 1993 *Liq. Cryst.* **15** 151
[18] Larson R G and Mead D W 1992 *Liq. Cryst.* **12** 751
[19] Manneville P and Dubois-Violett E 1976 *J. Phys.* (Paris) **37** 285
[20] Larson R G 1993 *J. Rheol.* **37** 175
[21] Wang J, Bhattacharya S and Labes M M 1991 *Macromolecules* **24** 4942
[22] Vermant J, Moldenaers P, Picken S J and Mewis J 1994 *J. Non-Newtonian Fluid Mech.* **53** 1
[23] Müller J A, Stein R S and Winter H H 1996 *Rheol. Acta* **35** 160
[24] Verment J, Moldenaers P and Mewis J 1994 *J. Rheol.* **38** 1571
[25] Ding J, Feng J and Yang Y 1995 *Polym. J.* **27** 1132
[26] Marruci G 1993 *Adv. Chem. Phys.* **86** 331
[27] Graziano D J and Mackley M R 1984 *Mol. Cryst. Liq. Cryst.* **106** 103
[28] Mather P T, Pearson D S and Larson R G 1996 *Liq. Cryst.* **20** 527
[29] Guan R H and Sun Y B 2006 *Chin. Phys.* **15** 1041
[30] Guan R H and Yang G C 2003 *Chin. Phys.* **12** 1283
[31] Zhang Z D, Yu H and Li L 2001 *Chin. Phys.* **10** 645
[32] Zhu G Z, Li H and Zhang W Z 1983 *Acta Phys. Sin.* **32** 845 (in Chinese)
[33] Lin L, Shu C, Shen J, Lam P M and Huang Y 1983 *Phys. Rev. Lett.* **49** 1335
[34] Lin L and Shu C Q 1984 *Acta Phys. Sin.* **33** 165 (in Chinese)
[35] Ding J and Yang Y 1998 *Macromolecules* **31** 176
[36] Yang Y, Luo K, Schmidt C and Peter C 2002 *Progress in Natural Science* **12** 188
[37] Gleeson J T, Palffy-Muhoray P and van Saarloos W 1991 *Phys. Rev.* A **44** 2588
[38] Xu G, Shu C Q and Lin L 1987 *Phys. Rev.* A **36** 277
[39] Lin L and Shu C Q 1984 *Acta Phys. Sin.* **33** 165 (in Chinese)
[40] Migler K B and Meyer R B 1993 *Phys. Rev.* E **48** 1218
[41] Büttiker M and Landauer R 1981 *Phys. Rev.* A **23** 1397
[42] Ding J and Yang Y 1994 *Rheol. Acta* **33** 405
[43] Ding J and Yang Y 1995 *Macromol. Symp.* **96** 135
[44] Ding J and Yang Y 1994 *Macromol. Symp.* **87** 115
[45] Chaikin P M and Lubensky T C 1995 *Principles of Condensed Matter Physics* (Cambridge: Cambridge University Press) p599
[46] Landau D L and Lifshitz E M 1958 *Quantum Mechanics* (Reading, MA: Addison-Wesley) p69
[47] Büttiker M and Thomas H 1980 *Phys. Lett.* A **77** 372